

SUPPORTING INFORMATION

Black Phosphorus/WS₂-TM (TM: Ni, Co) Heterojunctions for Photocatalytic Hydrogen Evolution under Visible Light Illumination

Eminegül Genc Acar ^{1,†}, Seda Yılmaz ^{2,3,†}, Zafer Eroglu ², İlknur Aksoy Çekceoglu ¹, Emre Aslan ⁴,
İmren Hatay Patır ^{1,*} and Onder Metin ^{2,3,5,*}

¹ Department of Biotechnology, Selçuk University, 42250 Konya, Turkey

² Department of Chemistry, College of Sciences, Koç University, 34450 Istanbul, Turkey

³ Koç University Tüpraş Energy Center (KUTEM), Koç University, 34450 Istanbul, Turkey

⁴ Department of Biochemistry, Selçuk University, 42250 Konya, Turkey

⁵ Koç University Surface Science and Technology Center (KUYTAM), Koç University, Istanbul 34450, Turkey

† These authors contributed equally to the work.

Instrumentation

Transmission electron microscope (TEM), scanning TEM high-angle annular dark field (STEM-HAADF), and energy dispersive X-ray (EDX) elemental mappings were recorded on an HT7800 TEM instrument with a STEM and EDX module working at 120 kV. An X-ray diffractometer (XRD) was used to detect the crystal structure of the samples, using a Bruker D8 Advance with a Cu K α radiation of 1.5406 Å. Photoluminescence spectroscopy measurements were documented with an Agilent Cary Eclipse PL using an excitation source of 320 nm. Lifetime analysis was performed with an Edinburgh Instruments FLS1000 spectrometer using a 377 nm laser source. Diffuse reflectance ultraviolet–visible–near infrared (UV–vis–NIR) spectroscopy (Shimadzu UV-3600 UV–vis–NIR spectrophotometer) was used to probe the photophysical properties of the samples. The surface composition and X-ray photoelectron spectroscopy (XPS) data were used for recording, with a Thermo Scientific K α X-ray photoelectron spectrometer with an aluminum anode (Al K α , 1468.3 eV).

The Materials Preparation

2.2.1. The preparation of crystalline BP and few-layer BP

BP crystals were synthesized via a well-established mineralization concept referred to as the chemical transport method. [1] In a typical synthesis process, 500 mg of red phosphorous, 20 mg of Sn, and 10 mg of SnI₄ were placed in a quartz ampoule. The ampoule was sealed under vacuum and heated up to 923 K with a heating rate of 1.35 °C/ min in a muffle furnace for 5h at this temperature. Subsequently, the furnace was cooled down to 773 K with a cooling rate of 0.33 °C/ min, and left to cool naturally. At the final step, the obtained big-size black crystals in the quartz ampoule were placed into toluene solution under an Ar gas atmosphere, and, after that, the ampoule was broken (caution: do not break the quartz ampoule in open air because it might catch fire). The yielded BP crystals were washed with ethanol several times to get rid of

the residual mineralizer. Eventually, the obtained BP crystals were transferred into a dark glass vial to inhibit light transmission and were kept under vacuum.

Preparation of few-layer BP: A specific amount of BP crystals was dispersed in DMF solution via sonication in a cooled ultrasonic bath ((Bandelin, 160/640 W, 35 kHz) for 8h, and the resulting dispersion was centrifuged at 2000 rpm for 15 min to remove the non-exfoliated BP. After the centrifugation, the resulting mixture was used for the synthesis of BP/WS₂ binary nanocomposites.

The Synthesis of BP/WS₂-TM (TM: Ni , Co) Ternary Nanocomposites

For the synthesis of ternary BP/WS₂-TM, the chemical reduction method was employed. In a typical synthesis process, the specific amount of BP/WS₂ binary nanocomposites was dispersed in 50 ml DMF solution via sonication for 1h. The clarified amount of transition metal precursor (nickel (II) acetate tetrahydrate, cobalt (II) acetate tetrahydrate, copper (II) acetate) was introduced into the BP/WS₂ dispersion. The obtained mixture was sonicated for 1 h and washed with ethanol at 9000 rpm for 10 min. The separated product was dispersed again in 16 ml DMF solution and transferred into a specially-designed four-necked glass reactor system which allows the chemical reduction synthesis to be performed under Ar gas flow with specific temperature control. The system was adjusted to 110°C and kept at that temperature for 30 min under gas flow. Subsequently, borane tert-butylamine complex dissolved in 2 ml of DMF solution was injected into the system. The mixture was kept for an additional 30 min at 110°C. The final suspension was cooled down to room temperature. The resulting suspension was centrifuged at 9000 rpm for 10 min, washed with ethanol, and dried under vacuum.

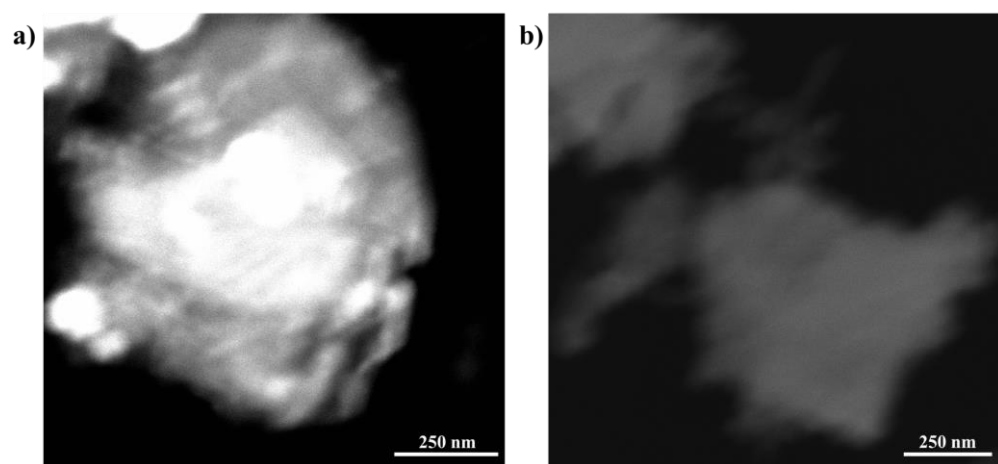


Figure S1. STEM images of (a) BP/WS₂-Ni (5%) and (b) BP/WS₂-Co (0.5%).

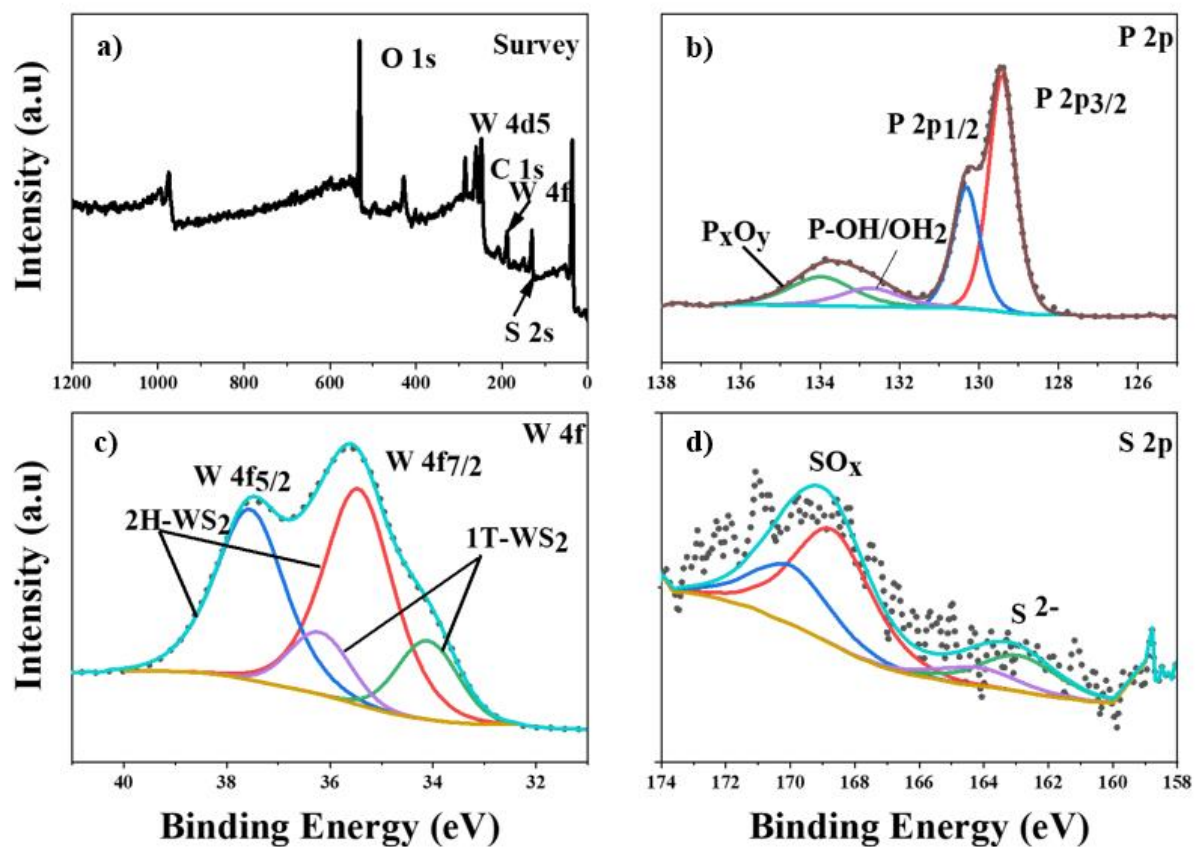


Figure S2. High resolution XPS spectra of BP/WS₂-25 binary nanocomposites: (a) survey, (b) P 2p, (c) W 4f, and (d) S 2p.

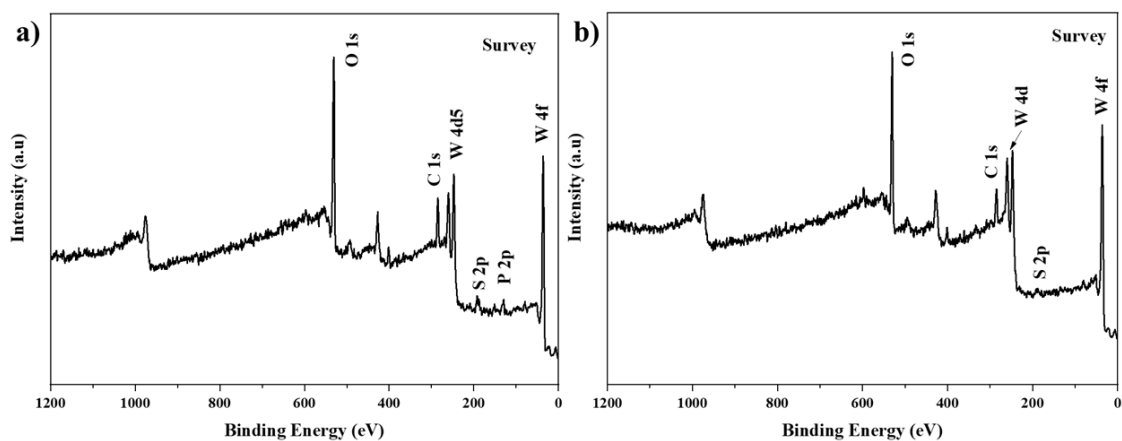


Figure S3. Survey spectra of (a) BP/WS₂-Ni (5%), and (b) BP/WS₂-Co (0.5%) nanocomposites.

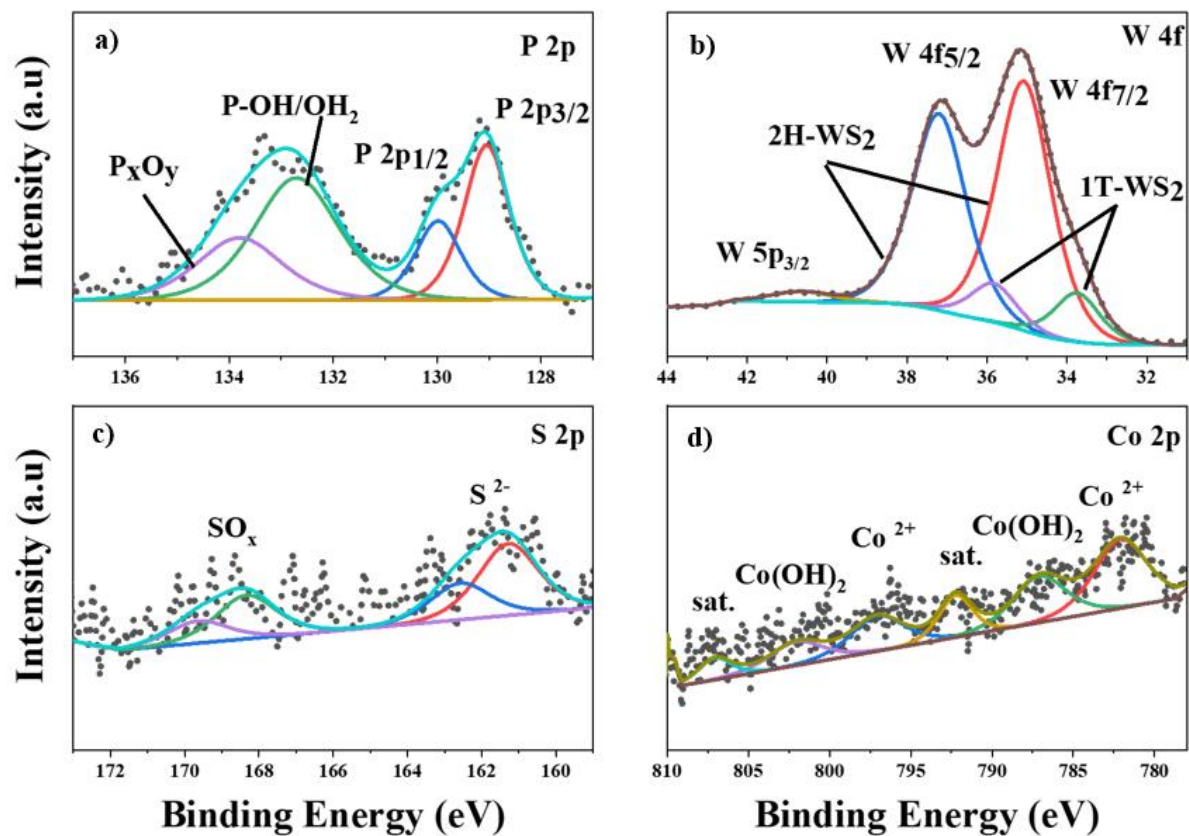


Figure S4. High resolution XPS spectra of BP/WS₂-Co (0.5%) nanocomposites: (a) P 2p, (b) W 4f, (c) S 2p, and (d) Co 2p.

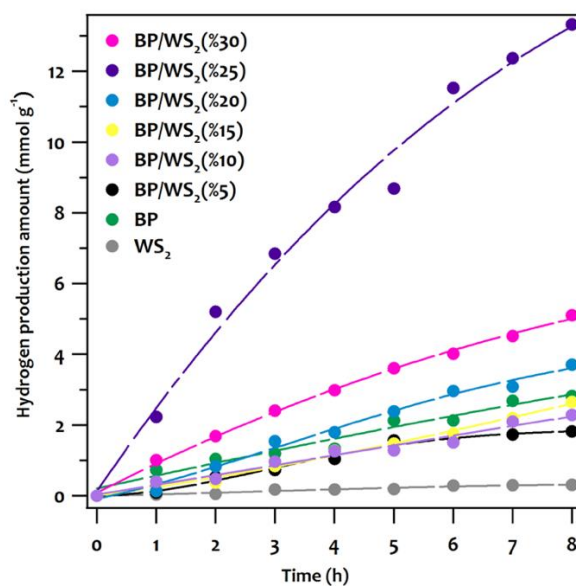


Figure S5. The BP loading effect on BP/WS₂ heterojunction by using different BP mass ratios in the presence of TEOA (0.33 M, 5%) and EY (3.25×10⁻⁴ M) as a sacrificial agent and sensitizer, respectively, under visible illumination (≥ 420 nm) for 8h.

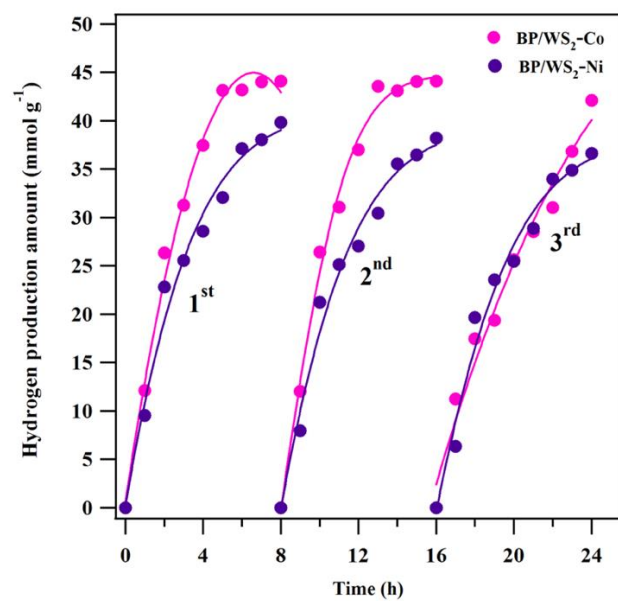


Figure S6. Stability study of hydrogen evolution over BP/WS₂-Ni and BP/WS₂-Co heterojunctions under visible light irradiation.

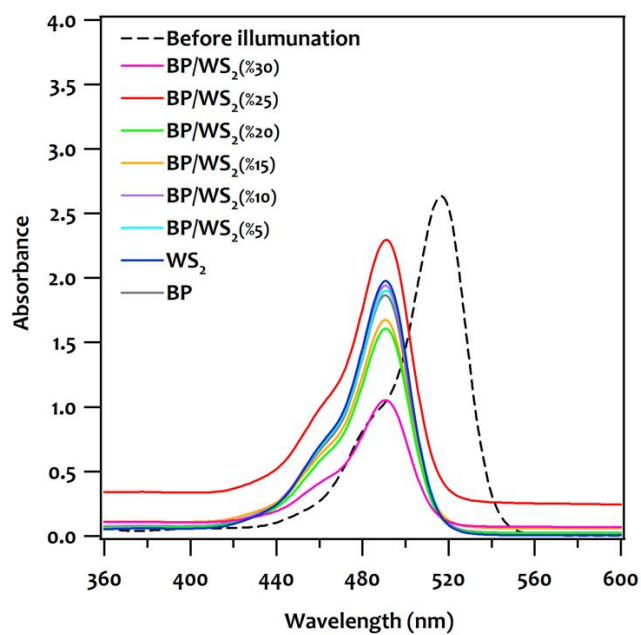


Figure S7. UV-vis spectra of BP, WS₂, and BP/WS₂ nanocomposites with different BP mass ratios in the presence of EY before and after photocatalytic reactions.

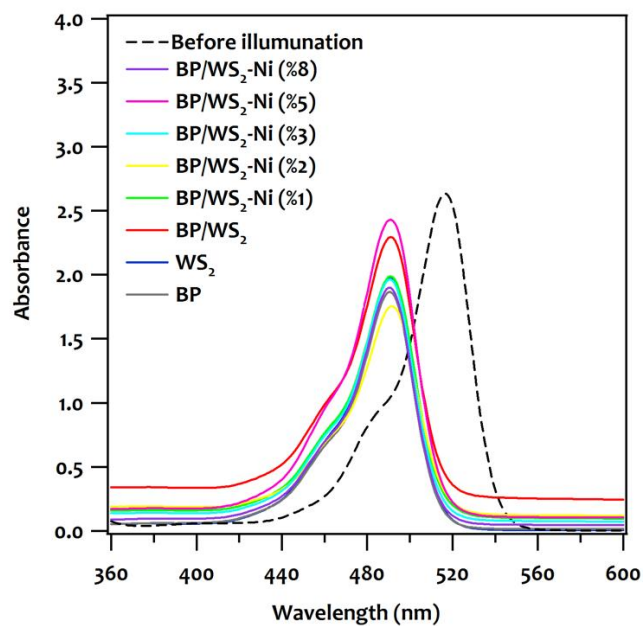


Figure S8. UV-vis spectra of BP, WS₂, and BP/WS₂ nanocomposites with different Ni mass ratios (from 1% to 8%) in the presence of EY before and after photocatalytic reactions.

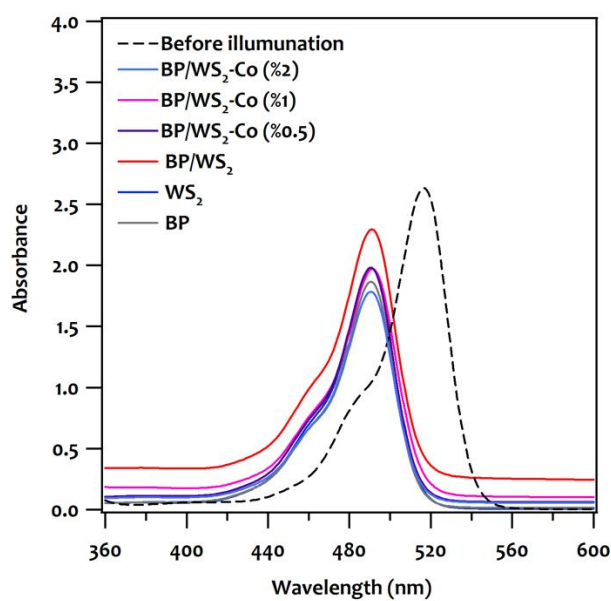


Figure S9. UV-vis spectra of BP, WS₂, and BP/WS₂ nanocomposites with different Co mass ratios (0.5%, 1%, and 2%) in the presence of EY before and after photocatalytic reactions.

Table S1. The comparison of BP/WS₂-TM; (TM: Ni, Co) heterojunction photocatalysts with similar materials that were tested in the photocatalytic HER in the literature.

Catalyst	The Amount of Hydrogen (mmol h ⁻¹ g ⁻¹)	Media	Ref.
BP/Pt	0.138	Methanol	[2]
CdS/BP	11.192	Lactic acid	[3]

BP/BiVO ₄	0.160	-	[4]
CoP/BP	0.694	Oxalic acid	[5]
MoS ₂ -BP/GO	3.467	Methanol	[6]
BP-MoS ₂	1.286	Na ₂ S/Na ₂ SO ₃	[7]
CdS/BP-MoS ₂	183.24	Lactic acid	[8]
BP/MoS ₂	0.5754	Na ₂ S/Na ₂ SO ₃	[9]
BP-NiO	0.1566	TEOA EY	[10]
BP/MoS ₂	3.9058	TEOA EY	[11]
BP/MoS ₂ -Ni	6.4139		
BP/MoS ₂ -Co	7.4282		
BP/WS ₂	2.2362	TEOA EY	This work
BP/WS ₂ -Ni	9.5264		
BP/WS ₂ -Co	12.1318		

References

1. Stan, M.C.; von Zamory, J.; Passerini, S.; Nilges, T.; Winter, M. Puzzling out the origin of the electrochemical activity of black P as a negative electrode material for lithium-ion batteries. *J. Mater. Chem. A* **2013**, *1*, 5293–5300.
2. Zhao, G.; Wang, T.; Shao, Y.; Wu, Y.; Huang, B.; Hao, X. A Novel Mild Phase-Transition to Prepare Black Phosphorus Nanosheets with Excellent Energy Applications. *Small* **2017**, *13*, 1602243.
3. Ran, J.; Zhu, B.; Qiao, S.-Z. Phosphorene Co-catalyst Advancing Highly Efficient Visible-Light Photocatalytic Hydrogen Production. *Angew. Chem., Int. Ed.* **2017**, *56*, 10373–10377.
4. Zhu, M.; Sun, Z.; Fujitsuka, M.; Majima, T. Z-Scheme Photocatalytic Water Splitting on a 2D Heterostructure of Black Phosphorus/Bismuth Vanadate Using Visible Light. *Angew. Chem., Int. Ed.* **2018**, *57*, 2160–2164.
5. Liang, Q.; Shi, F.; Xiao, X.; Wu, X.; Huang, K.; Feng, S. In situ growth of CoP nanoparticles anchored on black phosphorus nanosheets for enhanced photocatalytic hydrogen production. *ChemCatChem* **2018**, *10*, 2179–2183.
6. Zhu, M.; Fujitsuka, M.; Zeng, L.; Liu, M.; Majima, T. Dual function of graphene oxide for assisted exfoliation of black phosphorus and electron shuttle in promoting visible and near-infrared photocatalytic H₂ evolution. *Appl. Catal. B* **2019**, *256*, 117864.
7. Yuan, Y.-J.; Wang, P.; Li, Z.; Wu, Y.; Bai, W.; Su, Y.; Guan, J.; Wu, S.; Zhong, J.; Yu, Z.-T.; et al. The role of bandgap and interface in enhancing photocatalytic H₂ generation activity of 2D-2D black phosphorus/MoS₂ photocatalyst. *Appl. Catal. B* **2019**, *242*, 1–8.
8. Reddy, D.A.; Kim, E.H.; Gopannagari, M.; Kim, Y.; Kumar, D.P.; Kim, T.K. Few layered black phosphorus/MoS₂ nanohybrid: a promising co-catalyst for solar driven hydrogen evolution. *Appl. Catal. B* **2019**, *241*, 491–498.
9. Huang, Y.; Lu, H.; Wang, B.; He, W.; Dong, H.; Sui, L.; Gan, Z.; Ma, S.; Pang, B.; Dong, L.; et al. Synthesis and photocatalytic performance of MoS₂/Polycrystalline black phosphorus heterojunction composite. *Int. J. Hydrog. Energy* **2021**, *46*, 3530–3538.
10. Shi, L.; Wang, Y.; Yan, Y.; Liu, F.; Huang, Z.; Ren, X.; Zhang, H.; Li, Y.; Ye, J. Synergy of heterojunction and interfacial strain for boosting photocatalytic H₂ evolution of black phosphorus nanosheets. *J. Colloid Interface Sci.* **2022**, *627*, 969–977.
11. Yanalak, G.; Eroglu, Z.; Yilmaz, S.; Bas, S.Z.; Metin, O.; Patir, I.H. Metal doped black phosphorus/molybdenum disulfide (BP/MoS₂-Y (Y: Ni, Co)) heterojunctions for the photocatalytic hydrogen evolution and electrochemical nitrite sensing applications. *Int. J. Hydrog. Energy* **2023**, *48*, 14238–14254.